Design and Processing of Functionalized Epoxy Thin Films for Black Lipid Membrane Support and Testing

By

Evan Haning

Thesis

Submitted in partial satisfaction of the requirements for the degree of

Master of Science

in

Chemical Engineering

in the

OFFICE OF GRADUATE STUDIES

of the

UNIVERSITY OF CALIFORNIA

DAVIS

Approved:

_____

Tonya Kuhl, Chair

_____

Matthew Coleman

_____

Marjorie Longo

_____

Atul Parikh

Committee in Charge

2021

Table of Contents

Abstract

Black lipid membranes (BLMs) are a form of planar lipid bilayer suited for electrophysiological protein characterization. BLMs are typically formed on micromachined Teflon or patterned polydimethylsiloxane (PDMS). In this work, a BLM framework was fabricated using 1-3 µm-thick silanized epoxy thin-films. Thin-films were patterned with 50-500 µm-diameter pores using soft lithography on a low-cost cannabis oil extraction press. BLM formation with POPC lipid was confirmed using epifluorescent and confocal microscopy. BLMs were successfully formed in features of many different sizes. These results show that epoxy is a viable option to support BLMs, and suggests an opportunity for innovation in the field.

Acknowledgements

I would like to begin by thanking my major professor and mentor Dr. Tonya Kuhl. Coming from my previous experiences of professors never stepping foot in their labs, Dr. Kuhl's hands-on approach was game changing. Working directly alongside Dr. Kuhl in lab has been an incredibly valuable experience and I feel I have grown a lot. I want to sincerely thank her for her continuous support and positivity.

I would also like to thank my committee members Dr. Matthew Colman, Dr. Marjorie Longo, and Dr. Atul Parikh for their support and feedback on my work. Special thanks to Dr. Coleman for solving my BLM formation puzzle with the Teflon squeegee method!

Next, I would like to thank all the members of my research group: Deepshika Gilbile for training me when I first joined the group and for providing invaluable brainstorming sessions throughout my entire project, as well as laying the foundation for my design; Michael Bull and Tanner Finney for their continuous support, brainstorming, and help with anything and everything in lab.

Thank you to Dr. Michael Paddy for your immense help with confocal microscopy. Gathering that information would not have been possible without you.

Thank you to Dr. Jie Zheng and Shisheng Li for their amazing patience and help with electrophysiology measurements.

Also, thank you to Dr. Sean Gilmore for working with me at LLNL and teaching me about BLMs, as well as for training me on the Nanion Mini. I really appreciate all of your time and support.

Thank you to Mr. James Aldridge from Aditya Birla epoxies. Although I did not end up using your epoxy, your long-term communications were very helpful.

Finally, thank you to all of my friends and family for everything. I would not be here without all of you.

1 Introduction

1.1 The Lipid Bilayer for Biophysical Studies

Understanding cellular function, ranging from individual organelles to the cell as a working entity, has been a driving force in research since the cell's discovery in the 1600s [1]. As time has progressed and technologies have improved, so too has science's understanding of cells. Much of this was made possible by improved microscopy techniques, which allowed the scientists of the 1800s to actually observe cellular inner workings [2] and promoted the discovery of fundamental phenomena such as cell division. However, with these discoveries a problem became evident; cells are extremely complicated. All components of a cell interact with one another in some fashion. Therefore, in order to study the function of only one piece, it must be isolated from others [3]. Natural cell components are often isolated through centrifugation, which relies on density differences. However, this process is tedious and becomes increasingly difficult as organelles become closer in density. Issues such as this opened the door for artificial cells, which are generally easier to control and less fragile than their natural counterparts [4]. Creating an artificial cell from non-living chemical building blocks allows scientists to control the internal and external environments, in theory removing confounding interactions. Artificial cells can take the form of either complete cell analogues, which possess at least some of a cell's life-like properties (evolution, reproduction, etc.), or as mimics of individual cell structures [4]. For a complete cell analogue, the artificial cell must possess three key components: information, which is realized in the form of DNA; metabolism, which is a method of energy processing; and a compartment, which separates the interior of the cell from its environment [5].

In artificial cells, the compartment component has received the most research attention and is considered critical [6], [7]. In almost all living organisms, the cellular membranes satisfy the compartment requirement, with the phospholipid bilayer acting as the universal basis for membrane structure [8]. The phospholipid bilayer itself is very complex, however, even when decoupled from the rest of the cell: it is a

two-dimensional fluid inside of which individual lipid molecules can diffuse; it contains many different types of molecules, ranging from phospholipids, sphingolipids, cholesterol, and membrane proteins [8]; and all of these molecules interact with one another to form interconnected networks and complexes [9]. Phospholipid membranes are also often asymmetric, which reflects the different environments of the cell's interior and exterior. Because of these complexities and the importance of membranes as the location of much biological function, there is a clear motivation for the creation of synthetic lipid membranes to ease the study of their assembly, structure, and function. Synthetic bilayers also allow the isolation of specific membrane proteins, allowing their controlled study as well. In pursuit of this goal, two main classes of artificial bilayers are used: planar lipid bilayers and liposomes [10]. The chief difference between these two approaches is that planar lipid bilayers are flat sheets, while liposomes are liquid-containing spheres. There are a large number of subsets of planar lipid bilayers, all of which vary in their deposition method, supporting framework, tethering, etc. [11], [12]. Each subset has its respective pros and cons.

1.2 Black Lipid Membranes

One specific type of planar lipid bilayer is the black lipid membrane (BLM). In general, "BLM" describes a planar lipid bilayer that is formed in a pore between two chambers. These chambers generally contain aqueous buffer. In this location, the bilayer can act as an electrical barrier between both chambers. This enables direct probing of membrane electrical activity. These types of artificial bilayers are considered the closest analog to natural cell bilayers. This is because both sides of the bilayer are easily accessible, which allows for precise control of the formation conditions [9]. The earliest form of BLM was described in 1962 by Mueller et al. [13]. In this work, lipid bilayers were formed inside of a small Teflon pore (nominally 1 mm in diameter) submerged in an aqueous buffer. Upon application of a lipid in long-chain solvent, it was observed that a thinning process occurred spontaneously, resulting in an optically black bilayer film. A schematic view of this process is shown in Figure 1. This type of film formation is similar

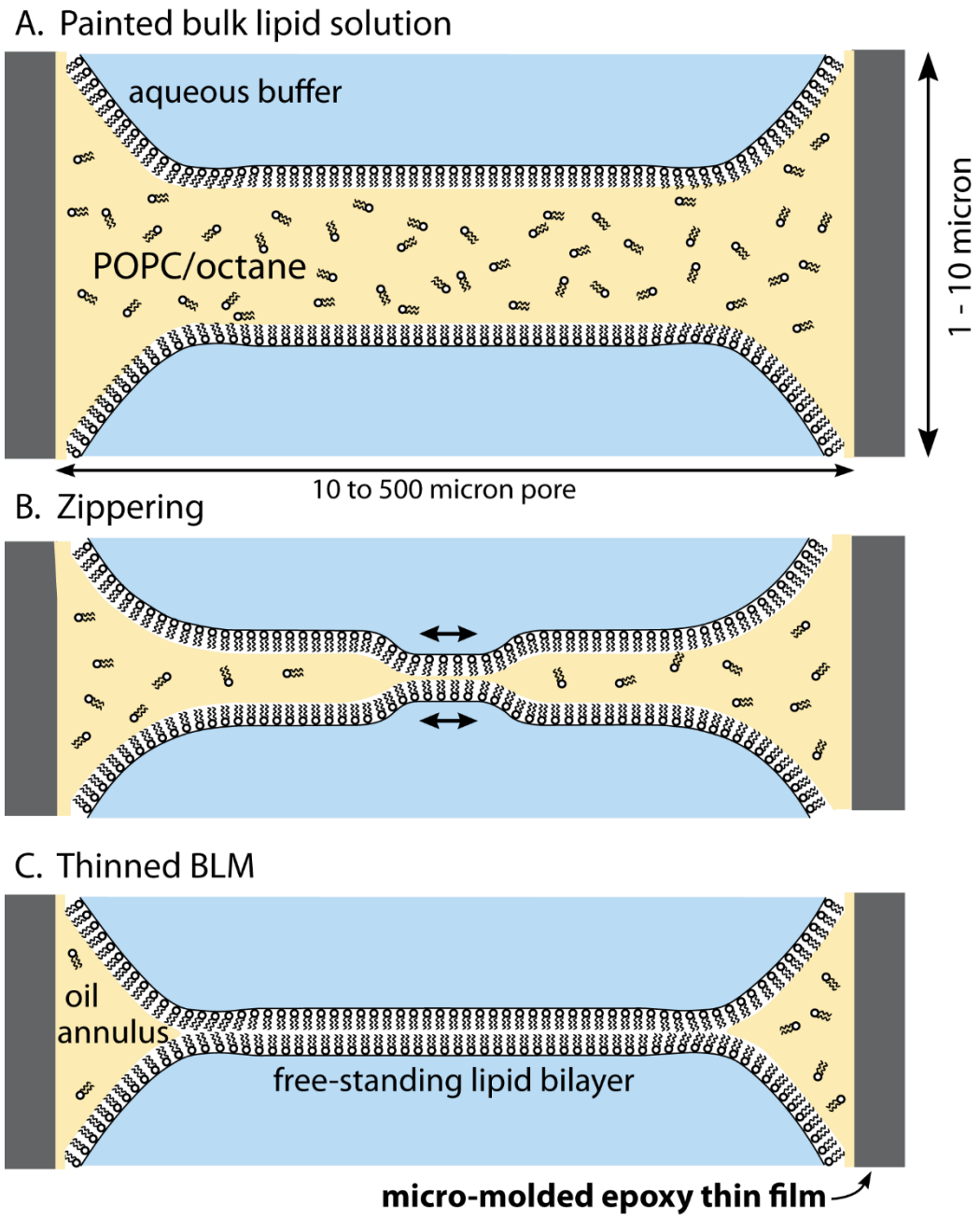

Figure 1: Schematic view of a BLM formation after the addition of lipid solution. A. Thick, bulk application of lipid solution. At this point no thinning has begun. B. Spontaneous nucleation of the membrane, often described as "zippering." This is seen visually in reflected light as the formation of a black area in the center of the pore that rapidly expands outward. C. Free-standing bilayer after thinning has stopped. This appears as a uniform black film in reflected light.

to "black film" descriptions made by Newton [14] and Hooke [15]. This similarity was the initial hint that the observed films were atomically thin; the eventual transition to black, rather than transparent, occurs due to destructive interference as the thickness of the film approaches the wavelength of visible light [16]. This pioneering method came to be described as the "painting" technique due to the requirement of

painting the lipid solution onto the Teflon surface with a small paintbrush or applicator. Membranes formed with this technique are considered to be "solvent-containing," meaning there is some amount of hydrocarbon solvent present in the bilayer itself [17]. Although this is not ideal for perfectly mimicking physiological conditions, it provides the advantage of keeping the membrane relatively soft and flexible. Central to the stability of these membranes is the presence of a hydrocarbon annulus around the rim of the pore [18]. This is required for the boundary conditions around the pore to be satisfied. However, the presence of hydrocarbon within the membrane itself is not required. As a result, research continued in a bid to find methods to form BLMs with little or no solvent. Several methods were discovered, including adapting Mueller's method for use with a non-partitioning solvent [19] and a folding method involving creating individual monolayers and raising them together to form a bilayer without painting, known as the Montal-Mueller technique [20]. Because the monolayers are formed individually and then brought together, the Montal-Mueller approach allows for easy asymmetric membrane formation. Although popular, this method requires specialized equipment to accomplish, namely a trough and dipper. This work will focus on painted, solvent-containing BLMs.

1.3 Previous Work

The basic process for solvent-containing BLM formation has not changed very much since its creation in the 1960s. This technique still mostly relies on painting lipid solution onto small apertures in hydrophobic polymers. Although this is a time-proven method, one of its central problems is a lack of scalability. Each pore is generally formed individually, often by micromachining [17]. This is a very time-consuming process because it involves manual removal of material on a pore-by-pore basis. This issue has led researchers to look for systems where pores can be fabricated or utilized en masse. One approach for such fabrication is to use photolithography (PL). PL has been used on silicon substrates to create large, ordered arrays of pores all at once. The method uses light and a transparency to pattern photoresist on the wafer, after which the unpolymerized photoresist is removed and the wafer is selectively etched [21]. PL on silicon also allows the creation of highly specific pore geometries, which can be changed to alter BLM

stability [22]. PL techniques have also been applied to thin polymer sheets, wherein an epoxy resist solution is used to etch away unwanted polymer [23]. Using these techniques, arrays of holes (often 1000s or more) can be created simultaneously [24]. This opens avenues for rapid BLM formation and higher throughput for membrane testing. However, manual painting of BLM arrays would be infeasible. Therefore, a method was devised to create BLMs through liquid flow. This technique usually involves alternating injections of lipid and buffer solutions through a channel such that the solutions pass over the pores [24]–[26]. This is akin to the "painting technique" since these BLMs are solvent-containing and created by direct application of lipid solution, but it removes the requirement of manual painting. This allows scaling of BLM systems and high throughput formation of BLMs.

In all PL methods, some form of deposition is necessary. This often requires many subsequent steps as well as final etching and development, making this a tedious process. An alternative to traditional PL is soft lithography (SL), which relies on elastomeric molds or stamps to create microstructures [27]. Unlike PL, SL generally does not require an etching process once the mold is made; when the desired material is deposited, the required shape can be formed directly with the mold. Often, this process comes in the form of hot embossing, where the desired material is deposited onto a surface and heated, and then the stamp is pressed onto the surface to make patterns. The patterns are very tunable, with various geometries and sizes feasible as long as the molds are available. In order to avoid the complexities associated with PL processes, SL will be the focus of this work.

Although less widespread than PL, there are several examples of SL applied to BLM fabrication. The majority of existing techniques utilize polydimethylsiloxane (PDMS) as the structural material. Often these techniques employ SU-8, a common rigid photoresist, as a mold. PDMS is then flowed or spin-coated around the mold to create microchannels. This allows the formation of single BLMs via hand-painting methods [28] or large numbers of BLMs using flow methods [26]. BLMs with lower solvent concentrations have also been made in machined PDMS channels [29], [30]. While the BLM in this case begins as solvent-containing, over time excess solvent will be absorbed by the PDMS due to its natural

solvent-partitioning properties. This technique allows the formation of Montal-Mueller-style BLMs without the need for a trough and dipper assembly.

While PDMS is well-suited to BLM fabrication due to its natural hydrophobicity, solvent partitioning properties, and availability of resources concerning its applications in soft lithography, it is not without its downsides. Although solvent partitioning can be useful, it can be a problem if the goal is to simply characterize proteins. Protein characterization can benefit from the "soft and flexible" nature of solvent-containing membranes [17]. Another potential issue is thickness. In current research, BLMs are formed with PDMS films 80-250 μm thick [28], [30]. While this does work, it has been shown that tapered or thinner pore edges can assist in increasing the stability of BLMs [22]. The exact mechanism behind this stability is not known, although we theorize it is related to smaller volumes of excess lipid solution in the pore annulus. While it is possible to spin coat thinner PDMS films, this requires the use of long spin times (>5 minutes) or solvent dilution [31]. Previous work in the Kuhl group has shown this is a non-trivial process and not reliably reproducible.

These problems present an opportunity for the use of a material other than PDMS as a BLM support. With the goal of using SL due to its simplicity and low cost, the new material must be a polymer. This polymer must also be easy to spin coat and have high resistance to long-chain solvents. Cross-linked epoxy meets all of these requirements. Due to the wide variety of low viscosity epoxies commercially available, there is a lot more freedom for the fabrication of thinner films with epoxy than with PDMS. Material properties, such as flexibility, opacity, and cure time, can also be modified by proper choice of epoxy.

2 Materials and Methods

Overview: BLM chip fabrication began with the creation of a silicon master. The transparency for the master is shown in Figure 2. After PL processing, the silicon master was then transferred to PDMS for use as a hot embossing stamp. The PDMS stamp was used with a consumer cannabis oil extraction press instead of a standard commercial hot embosser. This drastically reduced cost and made in-house fabrication straightforward. Commercial adhesive was used with poly(methyl methacrylate) (PMMA) to delaminate the embossed epoxy thin films and to support them. Silanization was used to prevent adhesion between the silicon master and the PDMS replica, as well as to achieve a hydrophobic surface on the epoxy films.

2.1 Materials

MilliQ deionized water from a Barnstead water purification system (Thermo Fisher Scientific) was used in all cases. Silanization protocols were conducted using (heptadecafluoro-1,1,2,2-tetrahydrodecyl)trichlorosilane (Gelest Inc.). Sylgard 184 Silicon Elastomer Kit (Dow Corning) was used for all PDMS applications. Polyvinyl alcohol (PVA) was used at MW 13,000-23,000 (Sigma-Aldrich) to spin coat sacrificial layers. A modified cannabis oil extraction press (Bubble Magic 5”x5” manual heat press) was used for all hot embossing. EpoxAcast 690 clear epoxy (Smooth-On Inc.) was used to create thin films. 1 mm thick PMMA sheets (Astra Products) with 0.05 mm thick adhesive backings (Adhesives Research MH-92712-3) were used to support the thin films. 1-palmitoyl-2-oleoyl-*sn*-glycero-3-phosphocholine (POPC, Avanti Polar Lipids, Inc.) was the central lipid used. N-hexane (HPLC ≥95%, Sigma-Aldrich) was used for the pre-paint solution, and n-octane (98+%, Alfa Aesar) was used for the painting solution. L-α-Phosphatidylethanolamine-N-(7-nitro-2-1,3-benzoxadiazol-4-yl) (Ammonium Salt) Egg-Transphosphatidylated, Chicken (Egg-NBD-PE, Avanti Polar Lipids, Inc.) and Texas Red™ 1,2-Dihexadecanoyl-*sn*-Glycero-3-Phosphoethanolamine, Triethylammonium Salt (TR-DHPE, Invitrogen)

were both used as fluorescent probes. NaCl (certified ACS, Fisher Chemical) and $CaCl_2 \cdot 2H_2O$ (99+% ACS, Sigma-Aldrich) were used for the buffer solution.

2.2 Fabrication of Silicon Master

SL fabrication of epoxy pores was based on PL of a silicon master. As shown in Figure 2, this allowed for many different aperture dimensions and densities to be explored quickly with 20 different 1.54 cm x 1.54 cm "chips." After designing the layout using AutoCAD, a transparency for PL was created by CAD Art

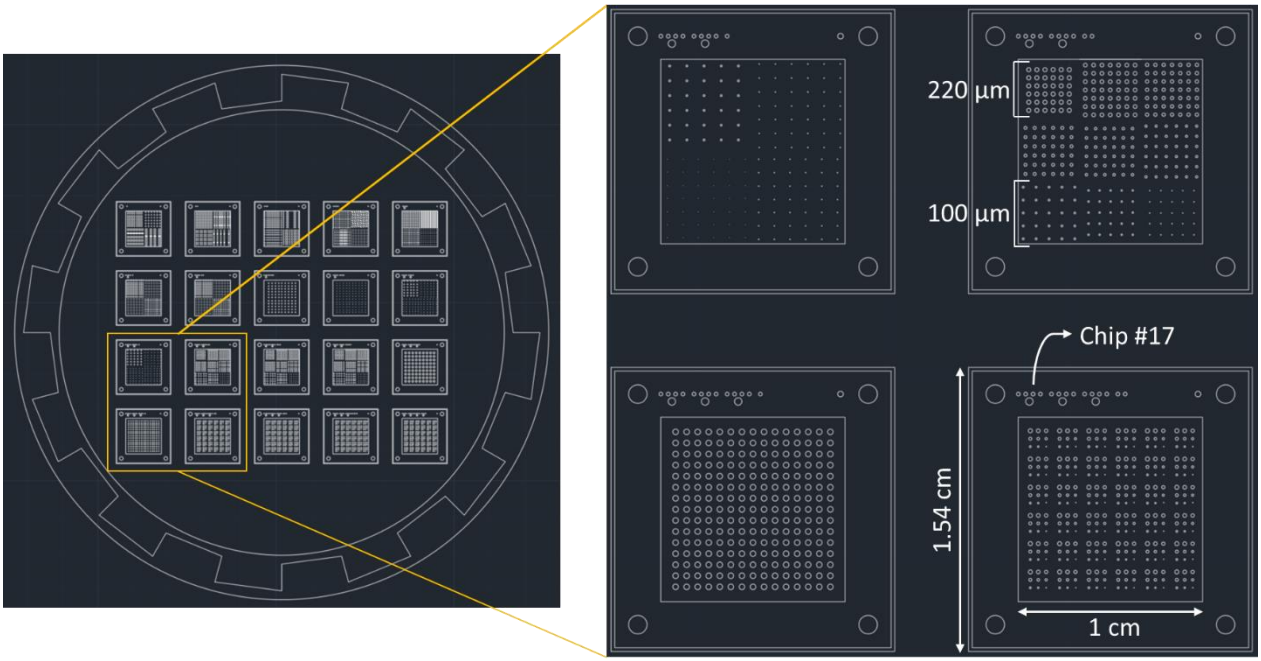

Figure 2: AutoCAD diagram of transparency. A negative photoresist was used, meaning all circular patterns formed pores on the master. Patterns range from 500 µm in diameter to 10 µm in diameter. The outer square pattern was designed as a cutting edge for easy film delamination. The dot patterns in the upper left corner of each chip are a key to recognize the chip number. Example pore diameters are provided for a sense of scale.

Services (Bandon, OR). This transparency was then used for standard reactive ion PL by Ravata Solutions (Davis, CA) to create the silicon master. Final depths of the circular pores were 9.7 µm, allowing for thin epoxy film patterning.

2.3 Silanization Protocol for Silicon and Epoxy Films

The material to be silanized was first activated using either UV ozone for 20 minutes (silicon wafers) or air (O_2) plasma for 1-2 minutes per side (epoxy chips). A standard desiccator was then prepped with a

stage wrapped in aluminum foil. Three small vial caps were wrapped in aluminum foil and placed onto the stage. The object to be silanized was placed in the middle of the stage, and each foil-wrapped cap was filled with approximately 0.25 mL of silane. The desiccator was then pumped under vacuum for 1 minute. After pump-down the desiccator was sealed and left for 1 hour, after which the object was removed. Silicon wafers were then baked on a hot plate for 30 minutes at 150°C to remove residual silanes. Epoxy chips were baked in an oven for 4 hours at 100°C to prevent warping.

2.4 PDMS Mold Fabrication

Silicon masters containing the reverse pattern desired were initially silanized according to the protocol shown above. An aluminum foil boundary was then applied around the edges of the mold to contain the PDMS. Care was specifically taken to fold the foil to ensure that no uncured PDMS would seep underneath the master. PDMS was vigorously mixed in a 5:1 ratio, with 40g of monomer and 8g of curing agent, and then allowed to degas under vacuum for 20 minutes. PDMS was then deposited onto the silanized wafer surface. The entire wafer was placed into a pressure chamber at 25 PSI for 10 minutes or until no bubbles were visible on the surface of the mold. The PDMS-coated wafer was then baked for 1 hour at 120°C. After curing, the PDMS was scored along the edges and carefully lifted away from the silicon master.

2.5 Hot Embossing and Film Delamination

Because epoxy forms a strong bond to silicon, Si wafers were first coated with a water-soluble sacrificial layer of PVA. A 5-inch silicon wafer was activated with UV ozone for 20 minutes. Approximately 3 mL of 0.22 μm-filtered 10 wt% PVA in water was deposited onto the wafer surface and spin coated at 1500 RPM for 60 seconds. This yielded a 550 nm ± 0.5 nm thin-film of PVA based on profilometry measurement. The wafer was then dried on a hotplate for 20 minutes at 100°C.

General inspiration for the embossing protocol was taken from work by Gel et al. [32]. Before embossing, the heat press was preheated to 65°C. A 6-inch Si wafer was covered with a single sheet of aluminum foil,

and the PDMS mold was placed feature-side-up onto the foil. During the preheat, the PVA-coated wafer was UV ozone treated for 10 minutes. Afterwards, approximately 8 mL of degassed epoxy was deposited onto the PVA-coated wafer and spin coated at 1200 RPM for 90 seconds. The epoxy was degassed under house vacuum for 20 minutes after mixing. Directly after spin coating, the wafer was placed epoxy-side-down onto the PDMS mold, and the entire mold sandwich was then placed into the heating press. The press was hand-tightened to the maximum pressure and allowed to heat for 1 hour. After, the sandwich was removed and the mold was separated. The embossed epoxy was then allowed to cure for a minimum of 1 additional day at room temperature. An example of the cured epoxy is shown in Figure 3. These approaches can be used with other epoxies successfully. Initial tests were conducted with TableTop Epoxy (Total Boat). However, this epoxy proved to be unsuitable due to its rapid cure rate and high viscosity (3500 cP when mixed). EpoxAcast 690 was selected because it was readily available, had a slower cure rate, and a low enough viscosity (280 cP when mixed) to be spin coated easily.

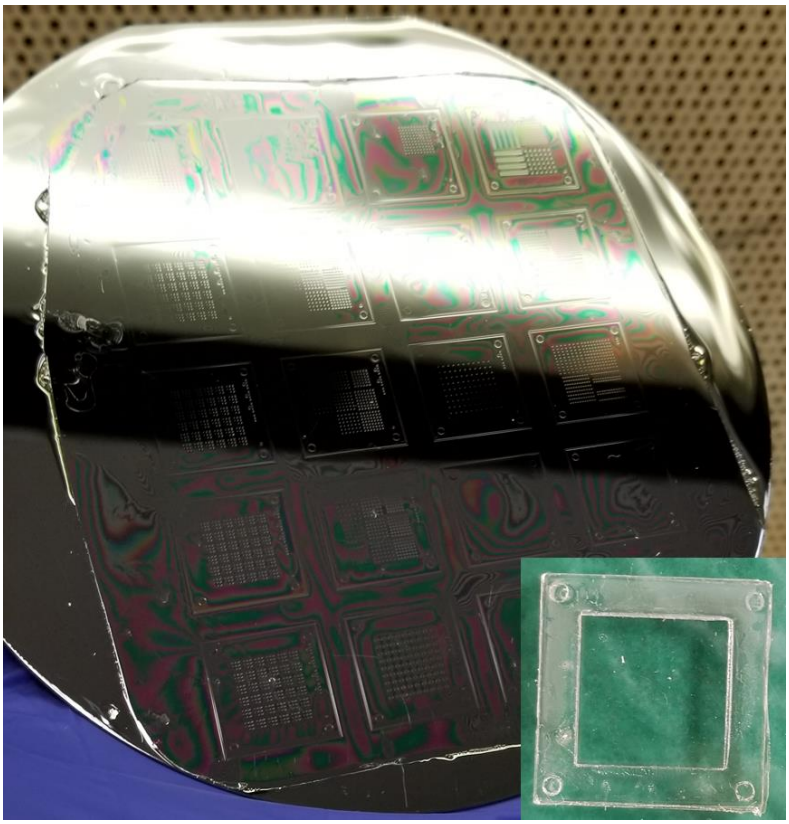

Figure 3: 5-inch silicon wafer with embossed Smooth On thin film. The inset image in the lower right corner shows a square PMMA frame, which would be attached to each square pattern on the silicon wafer for support.

After curing, laser-cut PMMA supports with adhesive backings were placed onto the pressed features (Figure 3 inset). A razor blade was used to score the outer edge of the PMMA supports, and the entire wafer was then soaked in DI water overnight to solvate and remove the PVA sublayer and thereby delaminate the supported epoxy thin-film. The PMMA-supported epoxy chips could then be easily removed and allowed to dry. Afterwards, the epoxy chips were then silanized as outlined previously and ready to be used.

Many different hole sizes were tested with the 20 different chip patterns. Due to limitations during the silicon master fabrication, patterns on the transparency <50 μm in diameter were not present on the silicon master, meaning they could not be embossed. However, this could be remedied with a new master in the future. Additionally, during the embossing process clean through-holes were not always made. Sometimes there was a thin residual spanning film over the pores. In this case, special care was taken during the O_2 plasma activation step of silanization to allow for adequate time for the residual film to burn off.

2.6 BLM Solution Preparation

Following standard BLM formation methods, the epoxy chips were first pre-painted with a lipid solution with 0.5 wt% POPC lipid dissolved in n-hexane. A painting solution for making the BLM was prepared with 99 mol% POPC and either 1 mol% Egg NBD PE or 1 mol% TR-DHPE in n-octane at 5 mg/mL. All lipid solutions were sonicated under gentle heat for a minimum of 2 hours before use. Buffer solution was 150 mM NaCl and 2 mM $CaCl_2 \cdot 2H_2O$ in DI water, as suggested by Beltramo et al. [33].

2.7 BLM Formation

The overall method for BLM formation was adapted from work previously published by Gutsmann et al. [17]. The silanized epoxy chip was first painted via paintbrush on both sides with a very small volume of pre-paint solution. The surface was allowed to dry for 20 minutes. A small regular or glass-bottom petri dish was then filled with approximately 5 mL of buffer. For rudimentary experiments, the regular petri

dish was used, along with two Teflon O-rings and double-sided tape to act as supports for the chip and to prevent it from touching the bottom of the dish. For confocal imaging, a glass-bottom dish was used. The epoxy chip was press-fit into the well at the bottom of the dish, and additional buffer was added to completely submerge the epoxy film.

Two approaches were utilized for painting. In the first, approximately 0.1 µL of painting solution was deposited onto the surface of the chip using a 0.5 µL syringe. A small Teflon strip/squeegee was then used to brush the lipid solution over the pores. This was facilitated using either brightfield or fluorescent microscopy. Brushing was repeated until visible thinning occurred in the form of black film or Newton's ring formation. In the second approach, a 10-µL pipette was used. The tip was inserted into the painting solution vial and approximately 1.5 µL of painting solution was aspirated back and forth. All solution was then emptied from the pipette tip, such that only a thin film remained. The tip was then submerged under the buffer solution and the plunger was depressed slightly to create an air bubble. This air bubble remained attached to the end of the pipette tip and acted as a brush. The air bubble was extended and retracted over the open pore a few times until a film appeared. This method was considerably gentler on the films than the Teflon squeegee method, as only an air bubble coated with painting solution made contact with the epoxy film surface. However, it was less suited for larger (>250 µm in diameter) pores due to limitations of the bubble size. Larger pipette tips may fix this issue.

2.8 Microscopy

BLMs were visualized using a Nikon Eclipse E600 upright epifluorescent microscope in both brightfield and fluorescent modes. Water immersion lenses were used, chiefly 40x (N40X-NIR, Nikon). Images were taken using an Andor Zyla 5.5 sCMOS scientific camera. NBD and TR fluorescent probes were imaged using standard FITC and TR fluorescent cubes, respectively. Image analysis was performed in NIS-Elements (Nikon).

Confocal microscopy was used to visualize and quantify BLM fluorescence. The 3i Marianas spinning disk confocal used in this work was purchased using NIH Shared Instrumentation Grant 1S10RR024543-01. We thank the MCB Light Microscopy Imaging Facility, which is a UC Davis Campus Core Research Facility, for the use of this microscope. Confocal image analysis was performed using ImageJ (FIJI). Image stacks were averaged using built-in FIJI Z-projection functions, and graphs were generated in Microsoft Excel.

3 Results and Discussion

Supported, patterned epoxy chips were successfully fabricated using the steps outlined in Section 2. Chip geometries were tailorable, and initial samples were created with a square shape. Circular PMMA supports were also used to fit in the glass-bottom petri dish wells for confocal microscopy measurements. Examples of the different chips are shown in Figure 4**.** Profilometry measurements showed an average epoxy film thickness of 1-3 µm, with some variability across the embossed surface (Figure). The variable thickness was caused by a combination of tilt on the PDMS mold and uneven pressure with the inexpensive hot press. A depression in the middle of the platens, causing the center to be thicker than the edges, is also a possibility. However, these variations in epoxy film thickness did not impact the chip functionality.

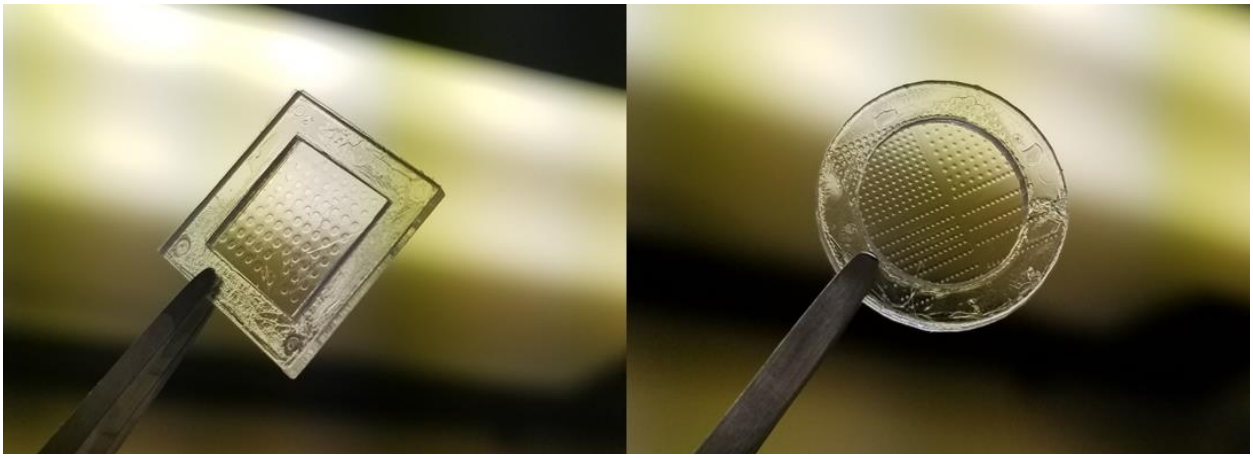

Figure 4: Examples of final silanized chips with free-standing, embossed epoxy film. The left chip is square and designed to contain an entire embossed pattern. The square chip contains 500 µm diameter pores. The interior side length is 10 mm. The chip on the right is circular and designed to be used with a glass-bottom petri dish. The circular chip contains 150 µm diameter pores in various patterns. The interior diameter is 9 mm.

Initial BLM formation testing was carried out using micromachined holes in 0.12 mm thick Teflon sheets simply made using 200 µm diameter drill bits. This platform was chosen for the first tests because it closely matched existing experimental literature, and was a good starting point for practicing BLM formation techniques. The resulting holes were imaged according to Section 2.8 Microscopy and are displayed in Figure. Since the films appeared optically black and possessed Newton's rings, it was assumed that they were in fact bilayers as described by Mueller.

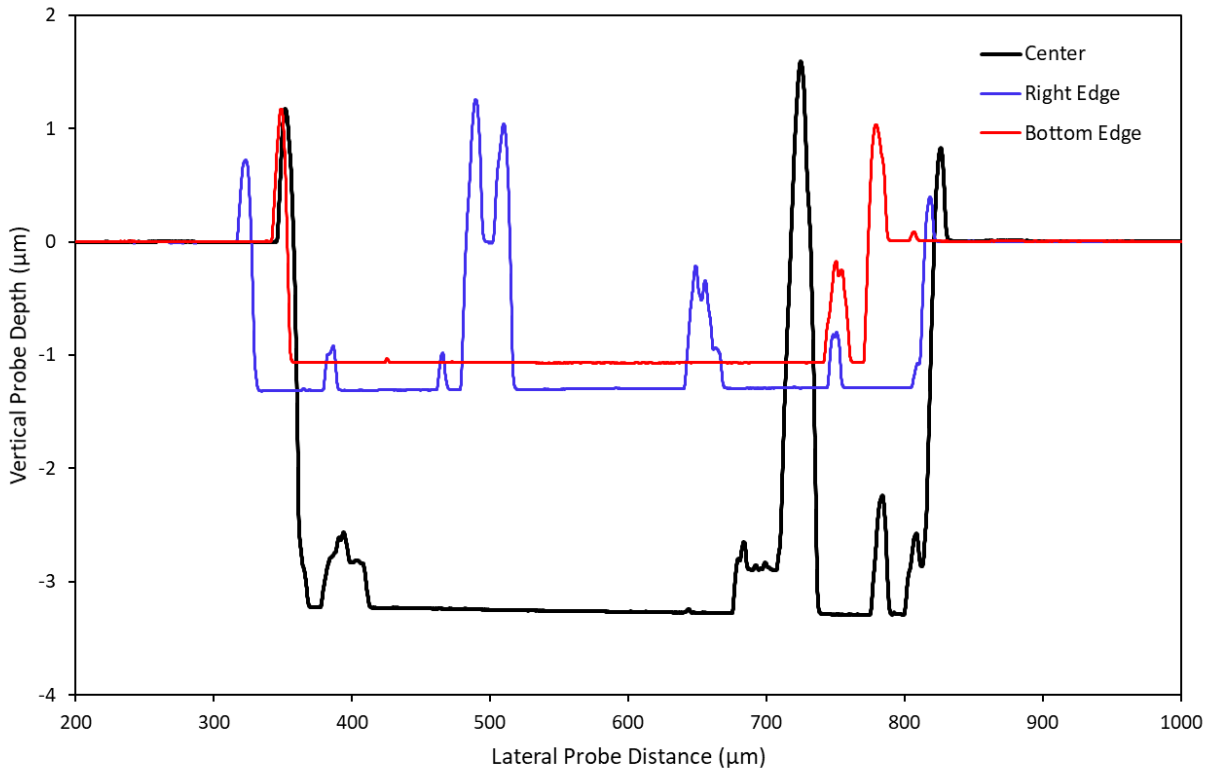

Figure 5: Profilometry data for hot-embossed Smooth On epoxy thin films on a 5-inch silicon wafer. Note the large variability in thickness between the center of the embossed wafer and the edges. The increased thickness in the center implies the presence of mold tilt or inconsistent pressure application.

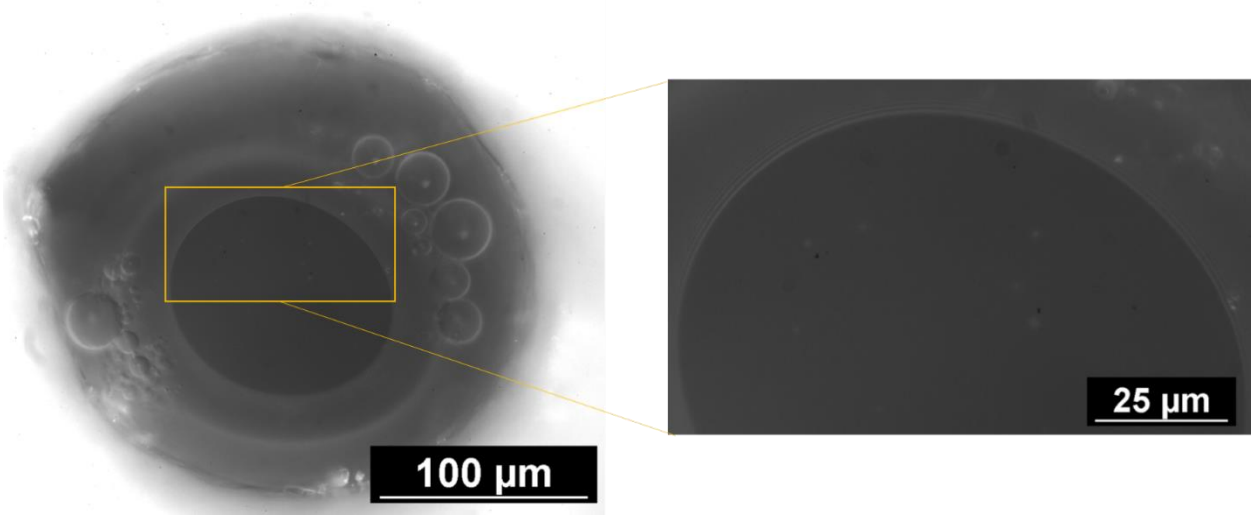

Figure 6: Brightfield image of POPC/Egg-NBD-PE BLM formed in a 200 µm diameter hole in thin Teflon film. Dark circular portion is the thinned BLM. Area with Newton's rings, as shown in the zoomed-in inset, is the solvent-rich annulus. Note the presence of air bubbles at the outer edges of the pore, which did not appear to significantly affect BLM formation.

BLM formation was also confirmed using a Nanion Orbit Mini. This off-the-shelf system allows direct electrophysiology measurements of BLMs on specially-designed MECA chips, which contain electrodes connected to apertures for BLM formation. Chips with 150 µm diameter pores were used. POPC painting solution with Egg NBD PE probe was used with the pipette-bubble method. The provided software confirmed that this painting solution and formation method produced BLMs with giga-ohm resistances and 4-6 pF capacitances, which are typical values confirming BLM creation according to Nanion literature.

After testing with machined Teflon films, formation methods were repeated using hot embossed epoxy thin-film chips. Regular epoxy is relatively hydrophilic and unsuitable for BLM formation. The advancing water contact angle of untreated epoxy films was 61°± 2° as measured with a goniometer. To render the films more hydrophobic, fabricated chips were silanized according to the protocol above. Advancing water contact angle was then >100°. BLM formation results were very similar to Teflon, with a black inner film gradually increasing in diameter and spreading over the pore in reflected light and Newton's rings appearing. A fluorescent image with 1% TR is shown in Figure 7. These BLMs did not

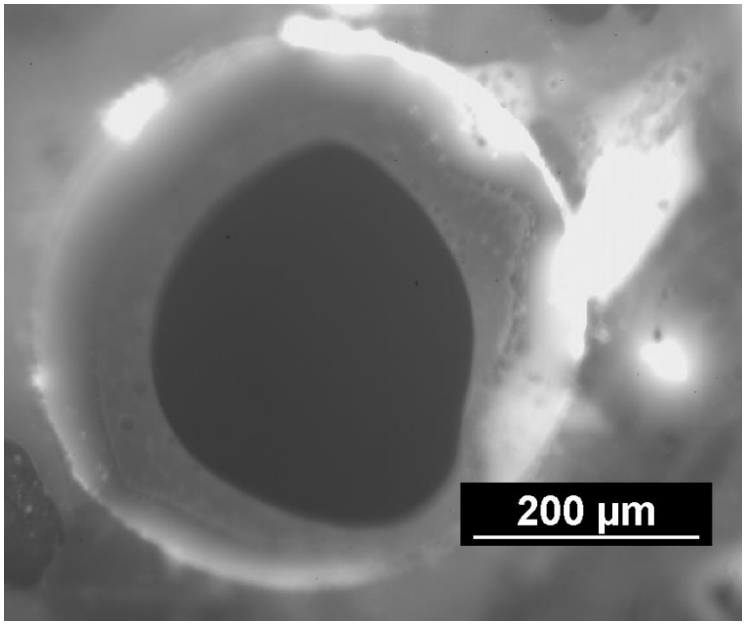

Figure 5: Texas Red fluorescent image of POPC/Tr-DHPE BLM formed in 500 µm pore in silanized Smooth On epoxy thin-film. Dark center shape is the thinned membrane, and brighter outer area is the solvent-rich annulus. Note that Newton's rings are not visible due to low magnification.

always form as perfect circles. There was some variability in the shapes without any clear cause. Additionally, there was a high amount of variability in their stability. Some BLMs would form (regardless of shape) and be resistant to bumps or vibrations of the petri dish while others would collapse at the slightest touch. Similarly, some BLMs appeared to last for several days, while others only survived for tens of minutes. There are several possible explanations for this behavior, such as particulate contamination or rough pore edges.

Fluorescent imaging proved to be a significant challenge using a standard epifluorescent microscope. There was high confidence that the observed structures were actually BLMs due to the presence of Newton's rings and the ability to see the thinning occur in real time. However, the dark membrane region did not show fluorescence appreciably above background levels due to excess painting solution around the pore, the bright annulus causing scattering, and the physical positioning of the BLM in the petri dish interfering with imaging [34]. Confocal microscopy was therefore used to quantify fluorescent intensity of the central membrane, as it allowed highly selective excitation of the BLMs to avoid these issues.

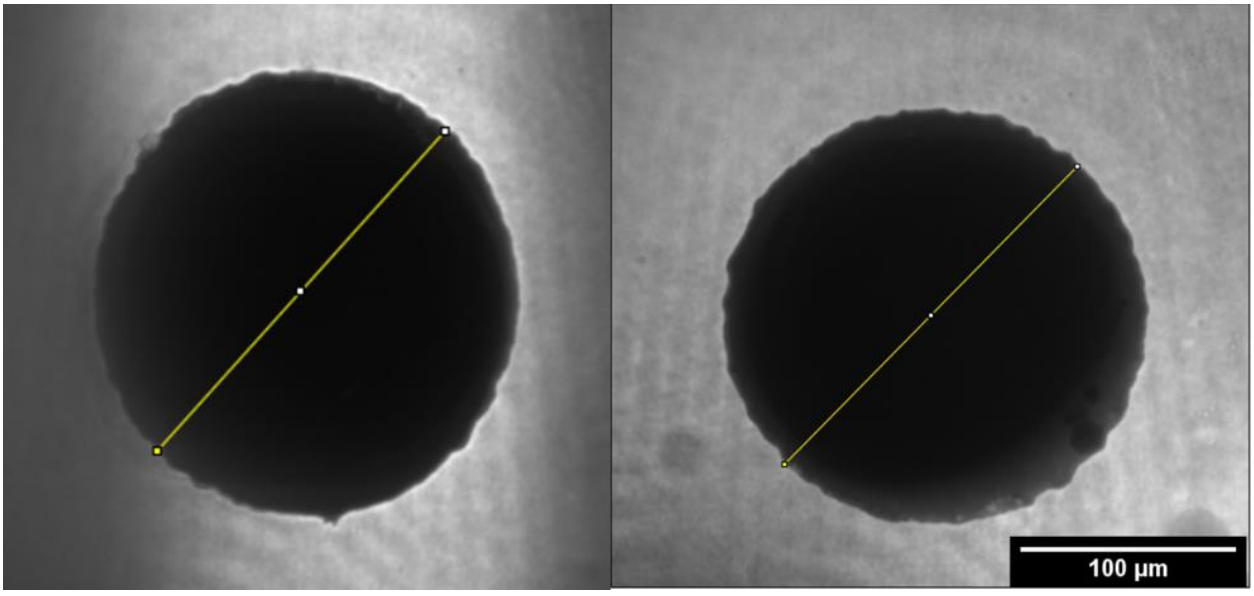

Figure 6: Confocal image stacks merged into a single, average image for line profile analysis. Both images were analyzed using the ImageJ "Average" algorithm. The left image is of an empty pore, while the right image is of a pore thought to contain a BLM. Both pores are 200 µm in diameter. BLM was formed using POPC/Egg-NBD-PE lipid mixture. The line is an example of how line fluorescence profiles were generated.

Confocal microscopy produced stacks of images probing the z-axis normal to the BLM plane. Pores with probable BLMs and empty pores were imaged to provide a comparison and ensure the BLM was fluorescing above the background level. In order to accurately create fluorescent intensity line profiles, the stacks needed to be averaged into a single, representative image. ImageJ provides several different algorithms to accomplish this. Figure 8 shows an example of this analysis. In all relevant cases, there was a distinct increase in fluorescent intensity of the BLM as compared to the blank pore captured at the same conditions. An example of a line profile is shown in Figure 9 with the "Average" algorithm used. This is strong evidence in favor of successful BLM formation.

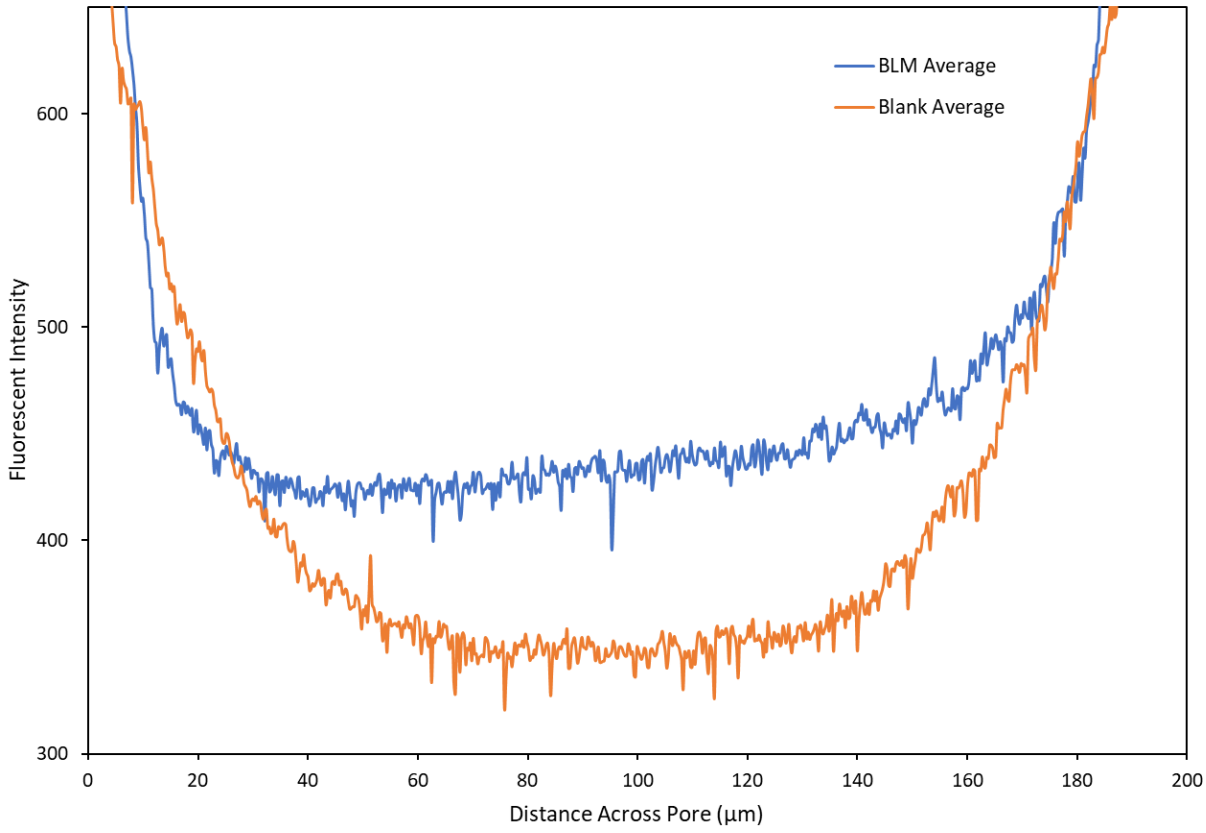

Figure 7: Fluorescent intensity levels for a 200 µm diameter suspected BLM and for a 200 µm diameter blank pore as analyzed with the "Average" z-projection algorithm in ImageJ. Both images were taken on the same day at the same imaging conditions. At the center of the pore (100 µm on the x-axis) it is clear the BLM has significantly higher intensity than the blank pore, strongly suggesting the presence of a fluorescent membrane. Similar results were found for all z-projection algorithms.

4 Conclusions and Future Work

Overall, this work presents a novel method for the fabrication of BLM supports. A silicon mold was fabricated and used to create PDMS replicates. These were used for hot embossing of epoxy thin films with a low-cost cannabis oil extraction press. Epoxy films were functionalized using silanes to hydrophobize the surface. White light, epifluorescent, and confocal microscopy demonstrated the successful formation of BLMs in the hot embossed pores. The epoxy thin films represent a new material and cost-effective means for fabricating ultra-thin BLM apertures in contrast to traditional Teflon or PDMS methods.

There are several areas for further exploration. First and foremost is exploring different types of epoxies. Smooth On was chosen mostly due to its low viscosity and easy availability. However, it is not the ideal material: it interacts negatively with the PDMS mold, occasionally sticking to it and eventually turning it white and destroying it. The reason for this interaction is not known, but other epoxies did not have these issues. Another issue with Smooth On (and most commercially available epoxies) is its hydrophilicity due to polar epoxy groups [35]. Because BLM formation requires the substrate to be hydrophobic, Smooth On must be activated with plasma and silanized. Although this does work, it significantly complicates the fabrication process. Moreover, the most expensive material for the fabrication is the silane. One potential approach to improve this would be the use of a hydrophobic cycloaliphatic epoxy (HCEP). These are relatively novel epoxies, but have entered commercial production. They are advertised to have low viscosity and very high water contact angle. If these properties are correct, this material is extremely promising for high-throughput BLM fabrication.

Another area for future study is microfluidics. The current hot embossing approach is very applicable for large scale BLM creation. Creating a microfluidic system that takes advantage of the large number of pores is straightforward using the PMMA frame and adhesive film to integrate flow channels. The film design outlined in this work is also compatible with microfluidic systems in the literature.

It would also be interesting to further experiment with the hot embossing process itself. There are other methods to create stamps that do not rely on patterning PDMS. One such possibility is to make a macro-scale stamp by placing the features by hand. In the case of simple circular holes this could be easily done with minutien pins, which are small (100-200 μm in diameter) pins used for biological dissection. A very rudimentary method would involve simply embedding a pattern of pins into a block of cured PDMS, and then using this as the stamp with the hot embossing machine.

Finally, it is essential to investigate single-pore recording, as BLMs are uniquely superior for this application in comparison to other artificial membrane types. Although not conclusive, there is evidence the films in this work are actually too thin to form a proper electrical seal. This could be due to either some form of current leakage through the epoxy or the presence of microholes in the film. A simple redesign of the transparency and mold with greater pore spacing and taller features would allow this system to be easily used for electrophysiology experiments on a single pore. This could range from simple membrane experiments to protein channel recording.

Works Cited

[1] L. John Wiley & Sons, Ed., *eLS*. Wiley, 2001.

[2] N. Bisceglia, "Cell Biology," *Nature*, 2014. [Online]. Available: https://www.nature.com/scitable/topic/cell-biology-13906536/.

[3] H. Lodish, A. Berk, and S. Zipursky, "Section 5.2, Purification of Cells and Their Parts," in *Molecular Cell Biology*, 4th ed., New York: W.H. Freeman, 2000.

[4] C. Xu, S. Hu, and X. Chen, "Artificial cells: from basic science to applications.," *Mater. Today (Kidlington).*, vol. 19, no. 9, pp. 516–532, Nov. 2016.

[5] R. V. Solé, "Evolution and self-assembly of protocells," *Int. J. Biochem. Cell Biol.*, vol. 41, no. 2, pp. 274–284, 2009.

[6] J. W. Hindley, R. V. Law, and O. Ces, "Membrane functionalization in artificial cell engineering," *SN Appl. Sci.*, vol. 2, no. 4, pp. 1–10, 2020.

[7] V. Noireaux, Y. T. Maeda, and A. Libchaber, "Development of an artificial cell, from self-organization to computation and self-reproduction," *Proc. Natl. Acad. Sci. U. S. A.*, vol. 108, no. 9, pp. 3473–3480, 2011.

[8] B. Alberts, A. Johnson, J. Lewis, M. Raff, K. Roberts, and P. Walter, "The Lipid Bilayer," in *Molecular Biology of the Cell*, 4th ed., New York: Garland Science, 2002.

[9] M. Zagnoni, "Miniaturised technologies for the development of artificial lipid bilayer systems," *Lab Chip*, vol. 12, no. 6, pp. 1026–1039, 2012.

[10] H. Ti Tien and A. Ottova-Letimannova, *Membrane Biophysics: As Viewed From Experimental Bilayer Lipid Membranes*, 1st ed. Elsevier Science, 2000.

[11] E. T. Castellana and P. S. Cremer, "Solid supported lipid bilayers: From biophysical studies to sensor design," *Surf. Sci. Rep.*, vol. 61, no. 10, pp. 429–444, 2006.

[12] R. P. Richter, R. Bérat, and A. R. Brisson, "Formation of solid-supported lipid bilayers: An integrated view," *Langmuir*, vol. 22, no. 8, pp. 3497–3505, 2006.

[13] P. Mueller, D. O. Rudin, H. Ti Tien, and W. C. Wescott, "Reconstitution of cell membrane structure in vitro and its transformation into an excitable system," *Nature*, vol. 194, no. 4832, pp. 979–980, 1962.

[14] I. Newton, *Opticks: Or, a Treatise of the Reflexions, Refractions, Inflexions and Colours of Light*. London: The Royal Society, 1704.

[15] R. Hooke, "Royal Society Meeting, 1672," in *The History of the Royal Society of London*, London: A. Millar, 1757, p. 29.

[16] M. Winterhalter, "Black lipid membranes," *Curr. Opin. Colloid Interface Sci.*, vol. 5, no. 3–4, pp. 250–255, 2000.

[17] T. Gutsmann, T. Heimburg, U. Keyser, K. R. Mahendran, and M. Winterhalter, "Protein reconstitution into freestanding planar lipid membranes for electrophysiological characterization," *Nat. Protoc.*, vol. 10, no. 1, pp. 188–198, 2015.

[18] S. H. White, D. C. Petersen, S. Simon, and M. Yafuso, "Formation of planar bilayer membranes from lipid monolayers. A critique," *Biophys. J.*, vol. 16, no. 5, pp. 481–489, 1976.

[19] S. H. White, “Formation of ‘solvent-free’ black lipid bilayer membranes from glyceryl monooleate dispersed in squalene,” *Biophys. J.*, vol. 23, no. 3, pp. 337–347, 1978.

[20] M. Montal and P. Mueller, “Formation of bimolecular membranes from lipid monolayers and a study of their electrical properties.,” *Proc. Natl. Acad. Sci. U. S. A.*, vol. 69, no. 12, pp. 3561–3566, 1972.

[21] D. Weiskopf, E. K. Schmitt, M. H. Klühr, S. K. Dertinger, and C. Steinem, “Micro-BLMs on highly ordered porous silicon substrates: Rupture process and lateral mobility,” *Langmuir*, vol. 23, no. 18, pp. 9134–9139, 2007.

[22] D. Tadaki *et al.*, “Mechanically stable solvent-free lipid bilayers in nano- and micro-tapered apertures for reconstitution of cell-free synthesized hERG channels,” *Sci. Rep.*, vol. 7, no. 1, pp. 1–10, 2017.

[23] M. El Khoury, T. Winterstein, W. Weber, V. Stein, H. F. Schlaak, and G. Thiel, “Photolithographic Fabrication of Micro Apertures in Dry Film Polymer Sheets for Channel Recordings in Planar Lipid Bilayers,” *J. Membr. Biol.*, vol. 252, no. 2, pp. 173–182, 2019.

[24] R. Watanabe, N. Soga, T. Yamanaka, and H. Noji, “High-throughput formation of lipid bilayer membrane arrays with an asymmetric lipid composition,” *Sci. Rep.*, vol. 4, pp. 1–6, 2014.

[25] B. Le Pioufle, H. Suzuki, K. V. Tabata, H. Noji, and S. Takeuchi, “Lipid bilayer microarray for parallel recording of transmembrane ion currents,” *Anal. Chem.*, vol. 80, no. 1, pp. 328–332, 2008.

[26] S. Ota, H. Suzuki, and S. Takeuchi, “Microfluidic lipid membrane formation on microchamber arrays,” *Lab Chip*, vol. 11, no. 15, pp. 2485–2487, 2011.

[27] S. Thomas, P. Balakrishnan, and M. S. Sreekala, Eds., “3.3 Soft Lithography,” in *Fundamental Biomaterials: Metals*, 1st ed., Woodhead Publishing, 2018, p. 72.

[28] X. Ren *et al.*, “Design, fabrication, and characterization of archaeal tetraether free-standing planar membranes in a PDMS-and PCB-based fluidic platform,” *ACS Appl. Mater. Interfaces*, vol. 6, no. 15, pp. 12618–12628, 2014.

[29] N. Malmstadt, M. A. Nash, R. F. Purnell, and J. J. Schmidt, “Automated formation of lipid-bilayer membranes in a microfluidic device,” *Nano Lett.*, vol. 6, no. 9, pp. 1961–1965, 2006.

[30] S. Choi, S. Yoon, H. Ryu, S. M. Kim, and T. J. Jeon, “Automated lipid bilayer membrane formation using a polydimethylsiloxane thin film,” *J. Vis. Exp.*, vol. 2016, no. 113, pp. 1–8, 2016.

[31] J. H. Koschwanez, R. H. Carlson, and D. R. Meldrum, “Thin PDMS films using long spin times or tert-butyl alcohol as a solvent,” *PLoS One*, vol. 4, no. 2, pp. 2–6, 2009.

[32] M. Gel, S. Kandasamy, K. Cartledge, and D. Haylock, “Fabrication of free standing microporous COC membranes optimized for in vitro barrier tissue models,” *Sensors Actuators, A Phys.*, vol. 215, pp. 51–55, 2014.

[33] P. J. Beltramo, R. Van Hooghten, and J. Vermant, “Millimeter-area, free standing, phospholipid bilayers,” *Soft Matter*, vol. 12, no. 19, pp. 4324–4331, 2016.

[34] M. Tsemperouli, E. Amstad, N. Sakai, S. Matile, and K. Sugihara, “Black lipid membranes: Challenges in simultaneous quantitative characterization by electrophysiology and fluorescence microscopy,” *Langmuir*, vol. 35, no. 26, pp. 8718–8757, 2019.

[35] A. Palanisamy, N. V. Salim, J. Parameswaranpillai, and N. Hameed, “Water Sorption and Solvent Sorption of Epoxy/Block-Copolymer and Epoxy/Thermoplastic Blends,” in *Handbook of Epoxy*

Blends, Cham: Springer International Publishing, 2017, pp. 1097–1111.